XLIII CILAMCE
21–25, November, 2022
FOZ DO IGUAÇU – PR – BRAZIL

Influence of geometry on the strength of shear keys based on numerical analysis

Luan Reginato[1], Danilo Pereira dos Santos[2], José Anchiêta Damasceno Fernandes Neto[3], Ray Calazans dos Santos Silva[4],

[1,2,3,4] *Department of Structures, School of Engineering of São Carlos, University of São Paulo*
Av. Trabalhador Sãocarlense, 400, 13566-590, São Carlos – SP, Brazil
[1]luanreginato@usp.br, [2]danilopereira.eng@usp.br, [3]anchietafernandes@usp.br, [4]raycalazans@usp.br

Abstract. Shear keys are present in several precast elements, such as foundation sockets and beam-column connections. In the literature, several analytical formulations are observed to predict its resistance. However, the formulations do not consider the entire geometry of the shear keys. In this paper, numerical models in finite elements were used with the software ABAQUS® to calibrate the shear keys tested by Zhou et al. (2005) and Faleiros Júnior (2018). The influence of the key geometry and the concrete strength was evaluated through a parametric analysis and compared with the analytical formulations. The results showed which geometric parameters have more influence on the strength of the keys. Furthermore, the results indicated that analytical formulations are inappropriate for some geometries.

Keywords: Shear key, precast concrete, ABAQUS, numerical analysis, precast connection.

1 Introduction

The constituent structural elements of precast concrete structures (CPM) are produced separately and joined to consolidate the final geometry of the system during the assembly stage. Cast-in-place concrete (CML) can be used to effectively transfer forces in the finished structure, where the shear stresses are transmitted through the interface between the CPM and CML. The transmission efficiency of these stresses is given by the type of roughness present in the interface and the slip condition at the interface. When there is a slip, the interface strength can be separated into three parts: adhesion, friction, and mechanics. One of the ways to increase the mechanical strength of the interface is the introduction of regular grooves on the surface of the concrete element, called shear keys [1-2].
Several structural elements in the precast concrete industry are produced with shear keys. Figure 1 shows some applications, such as a) hollow core slabs, b) structural walls, c) precast bridge segments, and d) foundation sockets.

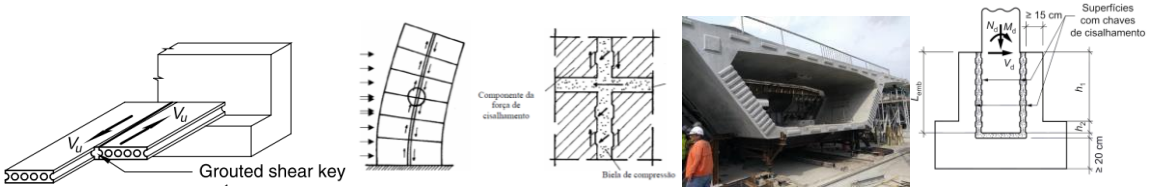

a) b) c) d)

Figure 1. Structural elements with the presence of shear keys. Source: [3] PCI (2010), [4] Van Acker (2002), [5] Smittakom (2019), [6] ABNT NBR 9062:2017

Shear keys are also used in beam-column connections, as indicated by typology 1 present in ABNT NBR 9062:2017 (Figure 2a) and Figure 2b, where two configurations of shear keys used in the column interface are presented.

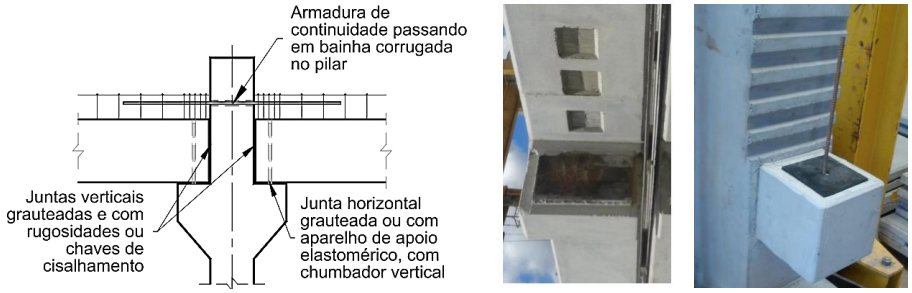

a) b)

Figure 2. Shear keys in beam-column connections in precast concrete structures. Source: [6] ABNT NBR 9062:2017

In the literature, there are two normative indications regarding the geometry of the shear keys. Figure 3a shows the indication of ABNT NBR 9062:2017, where two semi-waves together must measure up to 10 cm, and the tooth depth must be more than 1 cm with the inclination of the transition of the waves up to 45º. On the other hand, Figure 3b shows the indication of Model Code (2010), differing in the depth of the key (where values from 5 mm are allowed), the inclination angle (where suggested values up to 30º), and the projection length of the keys at the base, which in turn must not be greater than ten times the depth.

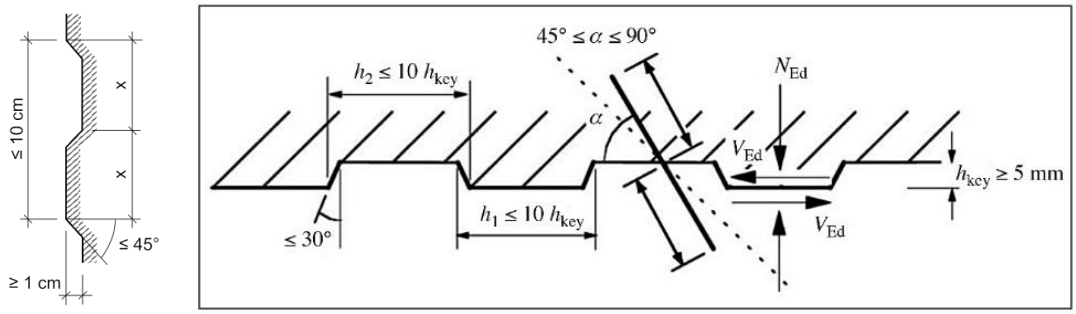

a) b)

Figure 3. Geometry of shear keys. Source: [6] ABNT NBR 9062:2017, [7] Model Code (2010)

According to Kaneko (1993), when the acting stress at the interface is close to the interface strength, a curvilinear crack is visualized in the compressed surface. With the increase in the load, there is an increase in the number of cracks until reaching the ultimate load, where there is a direct cut of the key base with the interconnection of these cracks, as shown in Figure 4a. Araújo (2002) highlights three types of failure: i) the base shear, as exemplified; ii) crushing of the concrete in the compressed region, generally occurring when the base length is large about the depth; and iii) accentuated slip between keys, generally occurring when the angulation is less than 45º, as shown in Figure 4b. When using shear keys with grout filling (Figure 4c), it is possible to visualize the appearance of diagonal cracks, suggesting the formation of compressive struts as a strength mechanism.

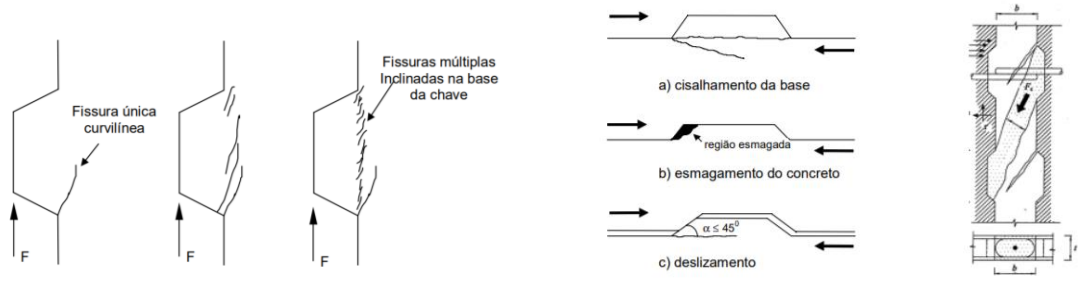

a) b) c)

Figure 4. Structural behavior and failure modes. Source: [8] Kaneko (1993), [2] Araújo (2002), [9] CEB FIB (2013, apud Faleiros Jr. (2018))

1.1 Analytical models

The interface shear strength force with shear keys can be estimated using several analytical models in the literature. Here, three semi-empirical models are presented:

- AASHTO (1999): $V = A_k \sqrt{6.792 \times 10^{-3} f_{cm}} (12 + 2.466\sigma_n) + 0,6 A_{sm} \sigma_n$
- Rombach e Specker (2004): $V = 0,14 f_{cm} A_k + 0,65 A_{joint} \sigma_n ; A_{joint} = A_k + A_{sm}$
- Turmo et al. (2006): $V = A_k \sqrt{f_{cm}} (0,906 + 0,1863\sigma_n) + 0,45 A_{sm} \sigma_n$

Where V is the interface shear strength force; A_k is the total area of the base of the keys; A_{sm} is the area of the base of the niches; σ_n is the normal compressive stress to the interface; f_{cm} is the compressive strength of concrete.
In the formulations, it is possible to visualize two strength portions, the friction portion, associated with the variable σ_n, and the mechanical strength portion of the keys (where σ_n does not interfere), linked to the f_{cm} root usually associated with the tensile strength of concrete. It is noticed that the analytical formulations disregard the geometric aspects of the shear keys and the projection area of the keys and niches. In this same context, this paper aims to investigate, through numerical analysis, the influence of geometry and the mechanisms involved in the interface strength force with shear keys.

2 Reference experimental test

The influence of geometry was investigated from the experimental test performed by Faleiros Júnior (2018), where the author studied the behavior of shear keys filled with grout to simulate the configuration of a precast beam-column connection. Figure 5a presents the geometry of the tested elements (composed of three parts), whose geometry of the shear keys (Detail 01) was indicated by ABNT NBR 9062:2017.
Figure 5b shows the element assembled for testing, where the joint length filled with grout is 30 mm. The average compressive strength of grout is 43.9 MPa, and that of precast concrete is 40.85 MPa. The external faces of the side pieces were restricted by concrete blocks, causing the confinement of the experimental test. The load was applied by force control on the upper face of the central part, and the vertical displacement was measured, as shown in Figure 5c. The author emphasizes that the test was finalized with the appearance of vertical and diagonal cracks, in addition to the limitation of the reaction apparatus. This way, the experimental test was completed before the rupture.

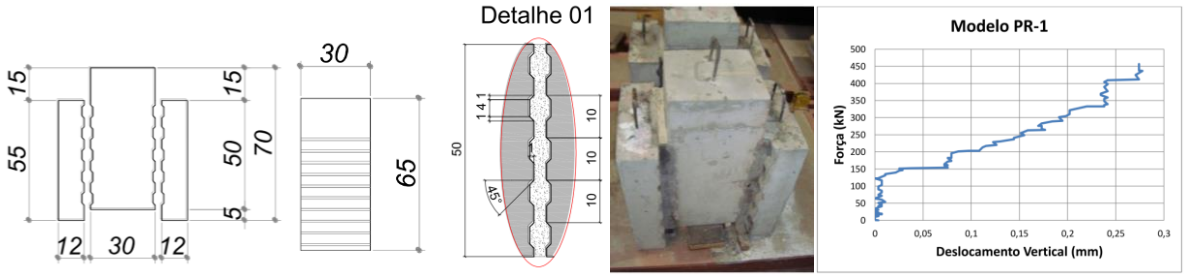

a) b) c)

Figure 5. Geometry, test setup, and results. Source: [9] Faleiros Júnior (2018)

3 Numerical analysis

The numerical analysis performed based on Faleiros Júnior (2018) will be presented in this section. Thus, the numerical model was calibrated, and the concrete geometry and strength were parameterized. The analyzes reported in this paper were conducted in Abaqus®.
A 2D model representing only half of the geometry was proposed to reduce the computational cost (Figure 6a). Figure 6b shows the mesh discretization in finite elements with an average size of 5 mm. The finite element chosen was the CPS4R which corresponds to the two-dimensional solid element in the plane stress state with four nodes and reduced integration. The CPS4R element has two translational degrees of freedom per node. Furthermore, Figure 6c presents the boundary conditions, with the vertical displacements constrained on the lower face.
As indicated in Figure 5, horizontal displacements were restricted on the left side to simulate confinement, according to Faleiros Júnior (2018). The symmetry condition was guaranteed with the restriction to horizontal displacements on the right side face. Finally, load application was simulated as a displacement of 1.2 mm on the top face.
The Hard-Contact, present in Abaqus®, was defined as the contact criterion. The Hard-Contact imposes the

following hypotheses: (i) only compression stresses are allowed; (ii) there is no penetration; (iii) surfaces can separate after contact. For the tangential behavior, the Coulomb friction model was inserted using a friction coefficient (μ) equal to 0.72 [10].

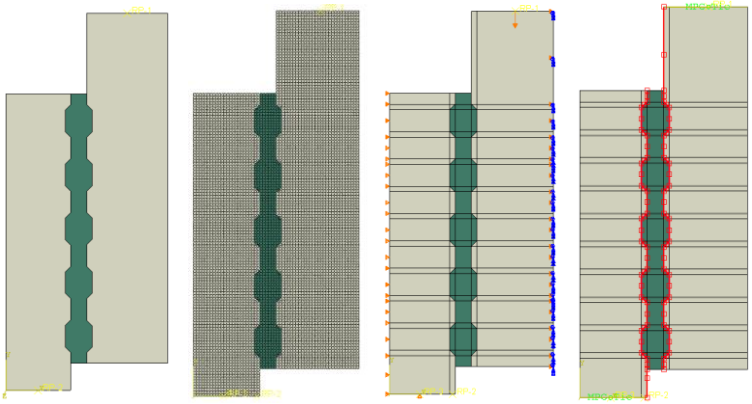

(a) (b) (c) (d)

Figure 6. Finite elements model: (a) Geometry; (b) Mesh; (c) Boundary conditions; (d) Hard-contact interface

In the experimental results of Faleiros Júnior (2018), only the grout was damaged. Therefore, the numerical model adopted a linear-elastic behavior to the lateral parts, using a Young's Modulus (E_c) of 30600 MPa. This module was calculated by formulating the Model Code (2010) (Table 1), where f_{cm} = 40.85 MPa. The grout behavior was described with the Concrete Damaged Plasticity (CDP), which is a non-linear model with plasticity and damage. The uniaxial tensile behavior was assumed to be linear until failure. Then, the ultimate tensile was calculated using the Model Code (2010) formulation, Table 1. Finally, the Hordijk (1992) formulation with fracture energy (G_F) of 0.1 N/mm was applied. For the compression behavior, a linear response was adopted up to 40% of the maximum stress (f_{cm} = 43.9 MPa). After 0.4f_{cm} and before the total $f_{cm,}$ a parabolic behavior was used, according to Eurocode 2 (2004) (Table 1). The post-peak behavior assumed was the formulation of Carreira and Chu (1985) with residual stress of 5 MPa.

Table 1. Analytical formulations

	Analytical Model
Model Code (2010) Young's modulus	$E_c = \alpha_i E_{ci}\ ;\ E_{ci} = 21500.\alpha_e \left(\frac{f_{cm}}{10}\right)^{1/3}\ ;\ \alpha_e = 1,0\ ;\ \alpha_i = 0,8 + 0,2\frac{f_{cm}}{88} \le 1,0$
Model Code (2010) Tensile strength	$f_{tm} = 0,3 f_{cm}^{\ 2/3}$
Hordijk (1992) HORDIJK, Dirk A. Tensile and tensile fatigue behaviour of concrete; experiments, modelling and analyses. Heron, v. 37, n. 1, 1992.	$\sigma_t(w) = f_{tm}\left\{\left[1+\left(c_1\frac{w}{w_c}\right)^3\right]e^{-c_2\frac{w}{w_c}} - \frac{w}{w_c}\left(1+c_1^3\right)e^{-c_2}\right\}$ $c_1 = 3\ ;\ c_2 = 6,93\ ;\ w_c = 5,14 G_F\ /\ f_{tm}$
Eurocode 2 (2004)	$\varepsilon_{c1}(‰) = 0,7 f_{cm}^{\ 0,31} \le 2,8$
Carreira e Chu (1985)	$\sigma_c(\varepsilon_c) = f_{cm}\left[\frac{\beta(\varepsilon_c/\varepsilon_{c1})}{\beta - 1 + (\varepsilon_c/\varepsilon_{c1})^{\beta}}\right]\ ;\ \beta = \frac{1}{1 - \frac{f_{cm}}{\varepsilon_{c1}E_{ci}}}$
Model Code (2010) Strain-stress equation for compression	$\sigma_c(\varepsilon_c) = f_{cm}\left[\frac{E_{ci}\frac{\varepsilon_c}{f_{cm}} - \left(\frac{\varepsilon_c}{\varepsilon_{c1}}\right)^2}{1 + \left(E_{ci}\frac{\varepsilon_c}{f_{cm}} - 2\right)\frac{\varepsilon_c}{\varepsilon_{c1}}}\right]$

The other coefficients that define the plasticizing surface, the plastic potential, and the visco-plastic behavior are shown in Table 2. Finally, the solution to the numerical problem was carried out using the Newton-Raphson

method.

Table 2. CDP plastic parameters

σ_{b0}/σ_{c0}	K_c	e	ψ	μ
1,16	0,667	0,1	38º	10^{-5}

3.1 Calibration Results

The experimental tests by Faleiros Júnior (2018) did not reach structural failure, so the maximum load was estimated using analytical models:

$A_k = 60 \times 300 \times 5 = 90.000\ mm^2$

$A_{sm} = 40 \times 300 \times 4 + 20 \times 300 \times 2 = 60.000\ mm^2$

$\sigma_n = 0\ MPa$

- AASHTO (1999) $V = 589.73\ kN$
- Rombach e Specker (2004) $V = 553.14\ kN$
- Turmo et al. (2006) $V = 540.50\ kN$

After the simulation, the maximum load found was 557.23 kN, which agrees with the analytical response.
Figure 7 shows the comparison between the cracking patterns. It is possible to notice a significant similarity in the presence of shear in the keys and also the inclined cracks. From the distribution of compressive stresses, it is noted that at the beginning of loading, there is the formation of compression struts in the corresponding keys at the same level.

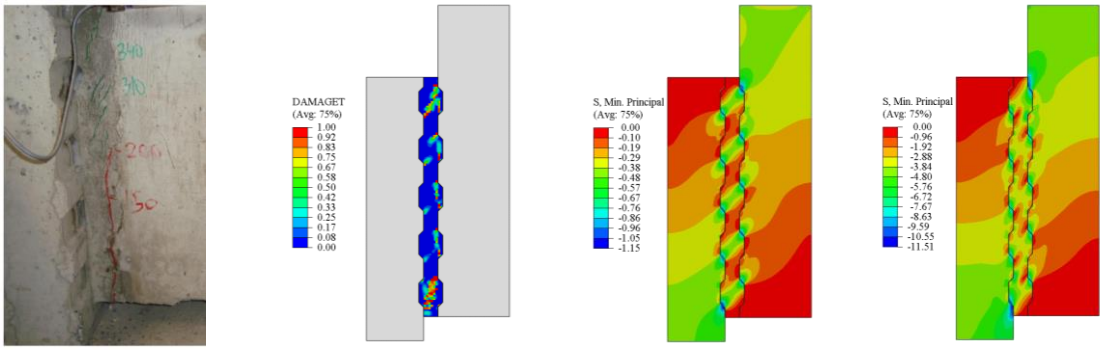

a) b) c) d)

Figure 7 - Comparison between a) experimental and b-d) numerical cracking patterns

Finally, when the load increases, there is a tendency for the strut to be formed starting from the upper key and leaning on the lower key, as seen in Figure 7d.

3.2 Additional simulation

In order to verify the validity of the constitutive model applied, three tests based on Zhou et al. (2005) were performed. Figure 8 presents the geometry, consisting of 3 keys. The width of the elements is 250 mm, and the strength of the concrete was varied accordint to Table 3.
Figure 8 shows the mesh discretization (5 mm) and the boundary conditions, where confining stress of 1 MPa was applied (Zhou et al., 2005). Figure 8 also shows the contact interface, which had the same properties as the previously simulated model. Only the material non-linearity of the keys on the right side was considered (colored green in Figure 8).

Figure 8 - Geometry of shear tests with keys

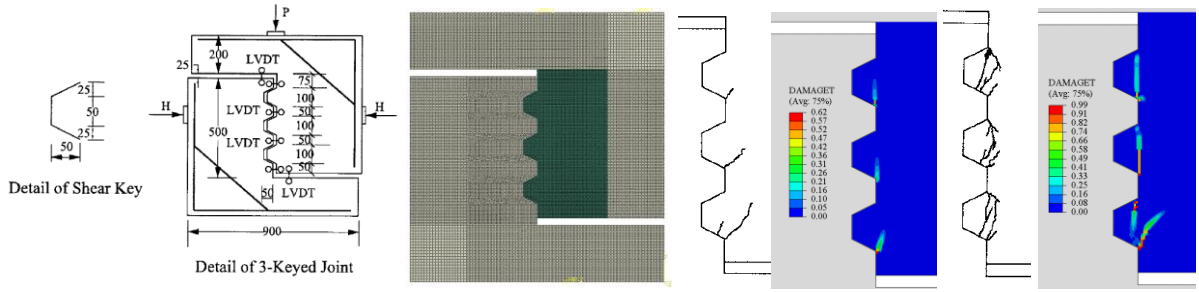

As can be seen in Figure 8, the cracking pattern was similar, with shear cutting in the keys. Finally, table 3 presents the specimen name, the concrete strength (f_{cm}), the maximum experimental load (V_{exp}), and the maximum numerical load (V_{num}). It should be noted that the numerical model estimated the failure load with a maximum error of 6.64%.

Table 3 - Results

Specimen name	f_{cm} (MPa)	V_{exp} (kN)	V_{num} (kN)	V_{exp}/V_{num}	Error
M1-D-K3-3	42.2	471	502.28	1.066	6.64%
M1-D-K3-2	35.2	437	452.27	1.035	3.49%
M1-D-K3-1	35.7	446	455.4	1.021	2.11%

4 Results

This evaluation aimed to estimate the impact of some parameters on the behavior of shear keys, such as joint length, key depth, key angle, number of keys, and key base length. In addition, the strength of the concrete was also varied, from 30, 43.9, and 50 MPa.

4.1 Length of the joint

Due to dimensional inaccuracies and location errors in the precast structural assembly, it is possible to have clearances between a beam and column faces. Therefore, this paper evaluates the behavior of keys with different joint lengths.

Figure 9a shows the geometry of the analyses, varying the length of the joint from 20, 30, 40, and 50 mm. Figure 9b shows the joint length and shear strength are proportional, with an average increase of 6.24% for every 10 mm.

Figure 9 – Parameterization results: (a) variation of joint length: 20, 30, 40, and 50 mm; (b) numerical result with joint length variation

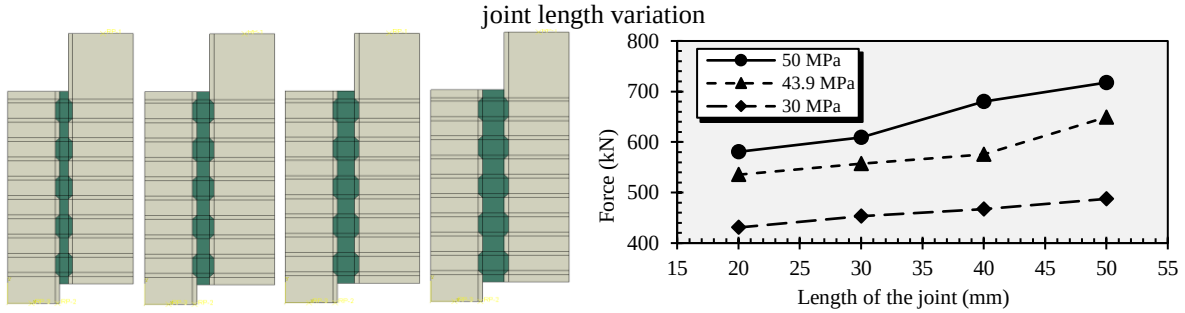

(a) (b)

Figure 10 presents that all failures have the same cracking pattern, i.e., through the shear of the keys. When analyzing the stress distribution, it can be seen that the longer the joint length is, the better defined the connecting strut will be.

Figure 10 - Cracking pattern and compressive stress distribution

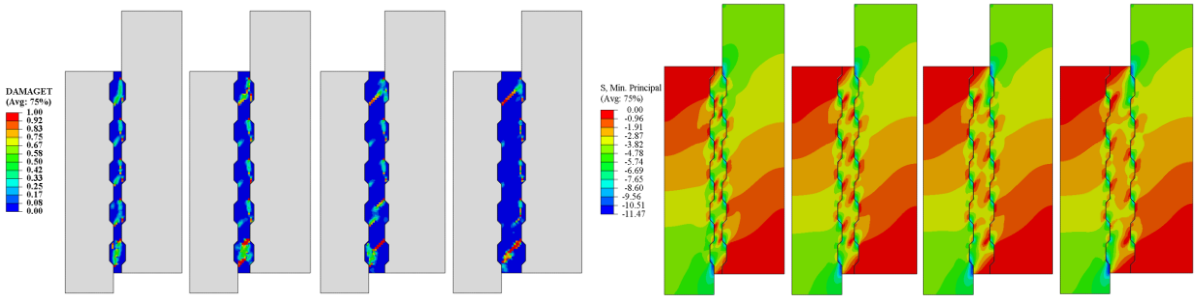

4.2 Depth and angle of keys

Figure 11a shows the variation in the depth of the keys (5, 10, 20, and 40 mm). Figure 11b shows the angulations evaluated for keys: 0º, 30º, 45º, and 60º.

Figure 11 – Parameterization results: (a) variation of key depth; (b) angle variation.

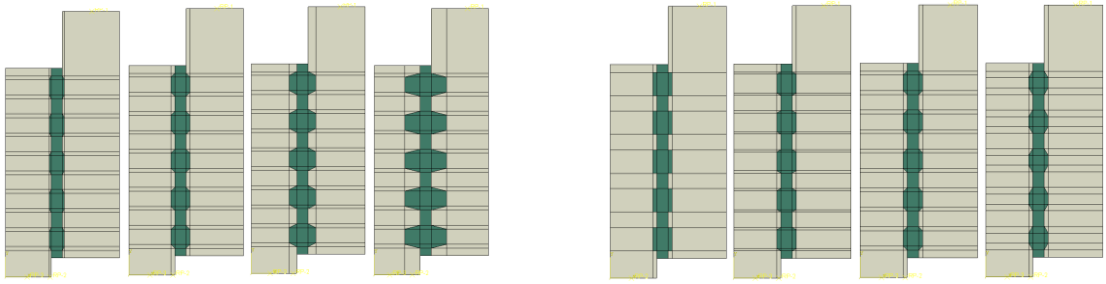

In Figure 12a it is observed that the depth and strength of the keys are proportional, with an average increase of 17% for every 10 mm (excluding the 5 mm depth data). Figure 12b shows the maximum load for the angle variation, where it was observed that the 30º angle presented a minimum strength.

The keys with a depth of 5 mm and keys with an angle of 60º presented a great slip; that is, they are less rigid. These two solutions have angles greater than 45º, which may represent an issue.

Figure 12 - Variation of (a) key depth and (b) angle

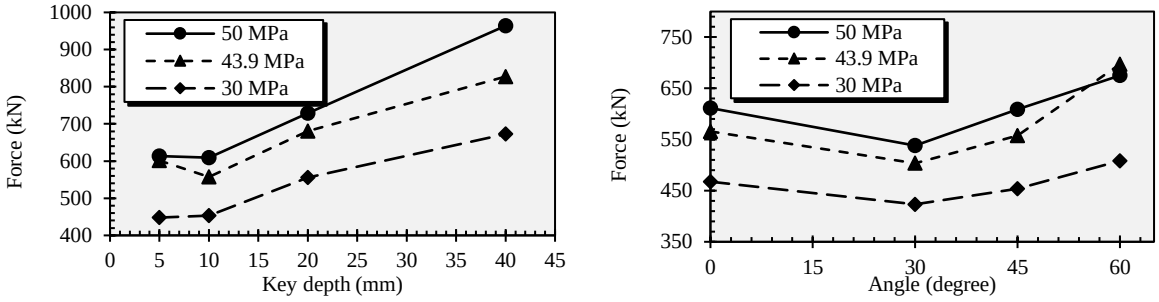

(a) (b)

Figure 13 shows the cracking pattern. It is possible to notice significant damage in the central region of the joint that grows with the depth of the key. About the angle, there is a difference in the location of the shear when the angle is 30º.

The compressive stresses are also shown in Figure 13. The same configuration of struts is noted, except for keys with a depth of 5 mm and an angle of 60º. In keys with a depth of 40 mm, a more defined strut for lower loads is seen, which justifies its greater strength.

Figure 13 - Cracking pattern: variation of key depth and variation of angle

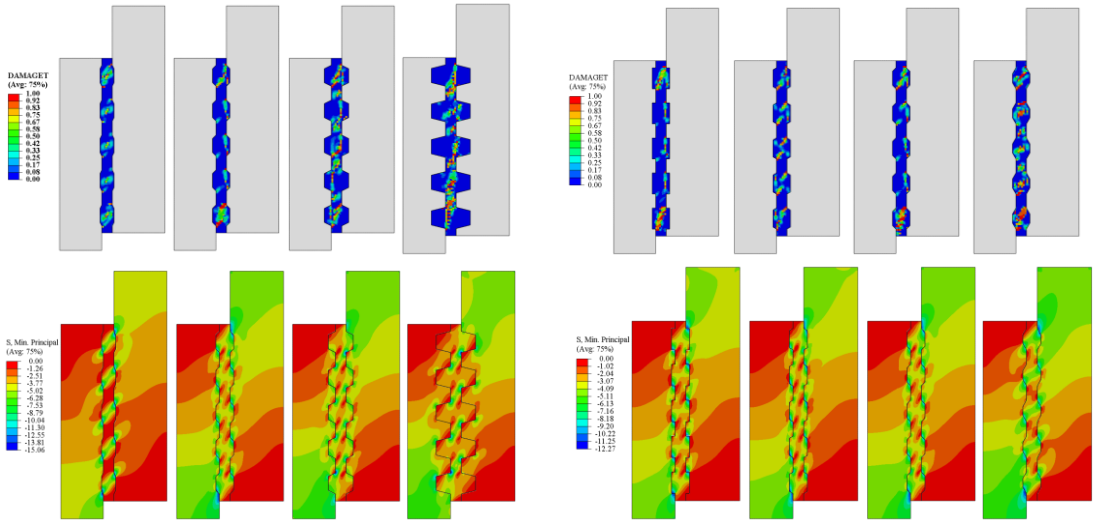

5 Conclusions

This paper presented an alternative for the numerical reproduction of connections by shear keys.
It is known that normative codes provide analytical solutions for estimating the strength of shear bonds. However, these solutions do not have to differentiate geometric particularities of the structural element. Thus, the solution presented by this article has great value as it represents a generic alternative to the analysis of connections strengths.
This study verified that the analytical formulations satisfactorily predict the ultimate load of the shear keys when compared with the experimental results. Furthermore, the same positive conclusion was extended to the numerical models proposed.
Numerical models also showed that the interface strength increases with the depth and length of the key base, the joint length, and the number of keys.
Future studies intend to explore the model presented in order to analyze more complex connections with the possibility of experimental validations.

Acknowledgements. The authors acknowledge the Department of Structures at the School of Engineering of São Carlos, where the numerical analysis was performed, and the funding provided by Coordenação de Aperfeiçoamento de Pessoal de Nível Superior – Brasil (CAPES) - Finance Code 001 and by CNPq (Brazilian government agency for research).

Authorship statement. The authors hereby confirm that they are the sole liable persons responsible for the authorship of this work, and that all material that has been herein included as part of the present paper is either the property (and authorship) of the authors, or has the permission of the owners to be included here.

References

[1] M. K. El Debs. Concreto Pré-Moldado: Fundamentos e Aplicações. Oficina de Textos, 2017.
[2] D. L. Araújo. Cisalhamento entre vigas e lajes pré-moldadas ligadas mediante nichos preenchidos com concreto de alto desempenho. PhD thesis (in portuguese), University of São Paulo, 2002.
[3] PCI Design Handbook. Precas and Prestressed Concrete: 7th edition. PCI, 2010.
[4] A. V. Acker. Manual de Sistemas Pré-Fabricados de Concreto (in portuguese). ABCIC, 2003.
[5] W. Smittakorn, P. Manavithayarak, P. Sukmoung. Improvement of shear capacity for precast segmental box girder dry joints by steel fiber and glass fiber. In: MATEC Web of Conferences. EDP Sciences, 2019. p. 04006.
[6] Associação Brasileira de Normas Técnicas. ABNT NBR 9062: Projeto e execução de estruturas de concreto pré-moldado. Rio de Janeiro, 2017.
[7] INTERNATIONAL FEDERATION FOR STRUCTURAL CONCRETE. CEB-FIP. Model code 2010: final draft. Lausanne: FIB, 2010.
[8] Y. Kaneko and V. C. Li, "Fracture behavior of shear key structures with a softening process zone". *International Journal of Fracture*, vol. 59, n. 4, pp. 345–360, 1993.
[9] J. H. Faleiros Júnior. Estudo experimental dos mecanismos resistentes das juntas com chave de cisalhamento em ligações pilar-viga. PhD thesis (in portuguese), Federal University of São Carlos, 2018.
[10] X. Zhou, N. Mickleborough, Z. Li, "Shear strength of joints in precast concrete segmental bridges". ACI Structural Journal, vol. 102, n. 1, pp. 3, 2005.
[11] D. J. Carreira and K. H. Chu, "Stress-strain relationship for plain concrete in compression". ACI Materials Journal, vol. 82, n. 6, pp. 797–804, 1985.